An Integrated Media, Integrated Processes Watershed Model – WASH123D: Part 7 – Sediment and Reactive Chemical Transport in Surface Runoff

FAN ZHANG[1], GOUR-TSYH YEH[2]

[1]*Environ. Sciences Division, Oak Ridge National Laboratory, Oak Ridge, TN, 37831, USA*
[2]*Dept. of Civil and Environ. Eng., Univ. of Central Florida, Orlando, FL, 32816, USA*

ABSTRACT

A watershed system includes river/stream networks, overland regions, and subsurface media. This paper presents a numerical model of sediment and reactive chemical transport in surface runoff of watershed systems. The distribution of mobile suspended sediments and immobile bed sediments is controlled through hydrological transport as well as erosion and deposition processes. Transport of M chemical species with a variety of chemical and physical processes is mathematically described by a system of M advective-dispersive-reactive transport equations. Decomposition via Gauss-Jordan column reduction of the reaction network transforms M species-transport equations into three sets of equations: a set of thermodynamic equilibrium equations representing N_E equilibrium reactions, a set of reactive transport equations of N_{KI} kinetic-variables involving only kinetic reactions (where N_{KI} is the number of linearly independent kinetic reactions), and a set of N_C component transport equations (where N_C is the number of components). The elimination of fast reactions from reactive transport equations allows robust and efficient numerical integration. The model solves the PDEs of kinetic-variables and components rather than individual chemical species, which reduces the number of reactive transport equations and simplifies the reaction terms in the equations. A hypothetical example was used to demonstrate the capability of the model in simulating sediment and reactive chemical transport subject to a complex reaction network involving both slow and fast reactions, under the effect of temperature. The widely used QUAL2E water quality model involving eutrophication is recast in the mode of a reaction network. Based on this eutrophication example, potential improvements over current practices using this model are addressed.

1. INTRODUCTION

Due to the rapid development of computer technology in the past two decades, water quality models play an increasingly important role in making environmental policy decisions for watershed management. A watershed system includes river/stream networks, overland regions, and subsurface media (Yeh, et al., 2005). This paper considers the sediment and reactive chemical transport modeling in overland water. The transport and transformation of water quality in river/streams and subsurface systems will be addressed in separate communications.

Most of the existing surface water quality models simulate either specific systems (Cerco and Cole, 1995; Shen et al., 2002; and Zheng et al., 2004) or systems containing specific reactions (Ambrose et al, 1993; and Bonnet and Wessen, 2001), which makes the application

of these models to more complicated biogeochemical processes in an overland region questionable. With better understanding and mathematical formulation of biogeochemical interactions, models considering interactions among chemicals based on reaction mechanism have a better potential for application to other systems (Steefel and Cappellen, 1998). No existing overland water quality model, to our knowledge, has used a fully mechanistic approach to estimate both kinetic and equilibrium reactive transport in overland water systems.

This paper presents a two-dimensional depth-averaged numerical model simulating the water quality in overland water systems. The main objective is to demonstrate the capability of the model in simulating sediment and reactive biogeochemical transport subject to both equilibrium and kinetic reactions. In our model, we include mobile suspended sediment particles scattered in water column and immobile bed sediment particles accumulated in water bed. There are six phases (suspended sediment, bed sediment, mobile water, immobile water, suspension precipitate, and bed precipitate phases) and three forms (dissolved chemicals, particulate chemicals sorbed onto sediments, and precipitates) for chemical species.

2. MATHEMATICAL BASIS

The distribution of bed and suspended sediment is controlled through hydrological transport as well as erosion and deposition processes (Gerritsen et al., 2000; Prandle et al., 2000; and Yeh et al., 2005). The temporal-spatial distribution of M chemical species with a variety of chemical and physical processes is mathematically described by the following advective-disperive-reactive transport equation.

$$\frac{\partial (h\rho_i C_i)}{\partial t} + \alpha_i L(\rho_i C_i) = hr_i \big|_N , \ i \in M \tag{1}$$

where h is the water depth; ρ_i is the density of the phase associated with species i, C_i is the concentration of species i, t is the time; $r_i \big|_N$ is the production rate of species i due to all N reactions, α_i is 0 for immobile species and 1 for mobile species, and operator L is defined as

$$L(\rho_i C_i) = \nabla \cdot (\mathbf{q}\rho_i C_i) - \nabla \cdot \left[h\mathbf{K} \cdot \nabla (\rho_i C_i) \right] - M_i^s \tag{2}$$

where $\mathbf{q}$ is the flux of overland flow; $\mathbf{K}$ is the dispersion coefficient; M_i^s is the source term of species i other than that due to reactions.

In a reaction-based formulation, $r_i \big|_N$ is given by the summation of rates of all reactions that the i-th species participates in,

$$r_i \big|_N = \frac{d(\rho_i C_i)}{dt} \bigg|_{reaction} = \sum_{k=1}^N \left[(\nu_{ik} - \mu_{ik}) r_k \right], \ i \in M \tag{3}$$

where ν_{ik} is the reaction stoichiometry of the i-th species in the k-th reaction associated with the products, μ_{ik} is the reaction stoichiometry of the i-th species in the k-th reaction associated with the reactants, and r_k is the rate of the k-th reaction.

Substituting equation (3) into equation (1) results in the transport equations of M chemical species described by

$$\frac{\partial (h\rho_i C_i)}{\partial t} + \alpha_i L(\rho_i C_i) = h \sum_{k=1}^N \left[(\nu_{ik} - \mu_{ik}) r_k \right], \ i \in M; \tag{4}$$

In a primitive approach, equation (4) is integrated to yield the distributions and evolutions of chemical species in a region of interest. However, when some fast equilibrium reactions

taking place in the system, this approach is not adequate (Fang et al., 2003). Here, we will take a diagonalization approach through decomposition. To avoid singularity of the reaction matrix, redundant reactions (i.e., fast reactions that can be derived from other fast reactions) are omitted from the system prior to decomposition. Define N_E as the number of linear independent fast reactions, N_{KI} as the number of linear independent slow reactions, N_{KD} as the number of dependent slow reactions, and $N_C = M - N_E - N_{KI}$ as the number of components. A complete Gauss-Jordan column reduction of the reaction network will transform the M species transport equations into three sets of equations: a set of N_E thermodynamic equilibrium equations describing N_E fast reactions, a set of N_{KI} reactive transport equations of kinetic-variables involving only slow reactions, and a set of N_C transport equations of components involving no reaction at all .

Algebraic Equations for Equilibrium Reactions

$$\frac{\partial(hE_i)}{\partial t} + L(E_i^{\ m}) = h\gamma_{kk}r_k + h\sum_{j \in N_{KD}} \gamma_{ij}r_j, k \in N_E, i \in M :$$

$$\frac{\partial(hE_i)}{\partial t} + L(E_i^{\ m}) \approx h\gamma_{kk}r_k = \infty \ \exists \ \begin{array}{l} \text{a thermodynamically} \\ \text{consistent equation} \end{array}$$

(5)

Reactive Transport Equations for Kinetic-Variables

$$\frac{\partial(hE_i)}{\partial t} + L(E_i^{\ m}) = h\gamma_{kk}r_k + h\sum_{j \in N_{KD}} \gamma_{ij}r_j, k \in N_{KI}, i \in M$$

(6)

Transport Equations for components

$$\frac{\partial(hE_i)}{\partial t} + L(E_i^{\ m}) = 0; \ \text{donating } T_k = E_i, \ k \in N_C, i \in M .$$

(7)

where E_i is the total concentration of a reaction extent, which is a linear combination of species concentrations, $E_i^{\ m}$ is the mobile part concentration of a reaction extent, and γ is the decomposed reaction matrix.

The elimination of fast reactions from reactive transport equations allows robust and efficient numerical integration. The model solves the partial differential equations of kinetic-variables and components rather than individual chemical species, which reduces the number of reactive transport equations and simplifies the reaction terms in the equations.

3. EXAMPLES

3.1 Overland transport with ten types of reactions

This example demonstrates capability of the model in simulating sediment and reactive chemical transport subject to both kinetic and equilibrium reactions, under temperature effect.

The domain of interest has covered a horizontal area of 5,000 m × 1,000 m and is discretized with 125 square elements (200 m × 200 m each). To focus on transport, water depth is set to be 2.0 m, and flow velocity is $V_x = 0.5$ and $V_y = 0.0$ m/s. In case 1, temperature is 15°C throughout the region; and in case 2, temperature ranges from 15°C to 25°C from the center of the domain to the top and bottom edges.

One size of cohesive sediment is taken into account with settling speed of 1.2×10^{-6} m/s, critical shear stress for deposition of 4.15 g/m/s^2, critical shear stress for erosion of 4.08 g/m/s^2, and erodibility of 0.1 g/m^2/s. Manning's roughness is 0.05. There are 14 species, including 3 dissolved chemicals in mobile water phase (CMW1, CMW2, and CMW3); 3

dissolved chemicals in immobile water phase (CIMW1, CIMW2, and CIMW3); 3 particulate chemicals sorbed onto suspended sediment (CS1, CS2, and CS3); 3 particulate chemicals sorbed onto bed sediment (CB1, CB2, and CB3); 1 suspension precipitate (SP3); and 1 bed precipitate (BP3). These species are considered to undergo ten types of reactions (Table 1).

TABLE 1. Chemical reactions considered in example 3.1.

Reaction and rate parameter	Type	No.
CMW1 + CMW2 ↔ CMW3 (k_{eq} = 0.4 m^3/g)	Aqueous complexation	R_1
CMW1+SS ↔ CS1 + SS (k_f = 0.0001 m^3/g SS /s, k_b = 0.0 s^{-1})	Adsorption or ion-exchange	R_2
CMW2+SS ↔ CS2 + SS (k_f = 0.0001 m^3/g SS /s, k_b = 0.0 s^{-1})	Adsorption or ion-exchange	R_3
CMW3+SS ↔ CS3 + SS (k_f = 0.0001 m^3/g SS /s, k_b = 0.0 s^{-1})	Adsorption or ion-exchange	R_4
CMW1+BS ↔ CB1 + BS (k_f = 0.00001 m^2/g BS /s, k_b = 0.0/h $m^{-1}s^{-1}$)	Adsorption or ion-exchange	R_5
CMW2+BS ↔ CB2+ BS (k_f = 0.00001 m^2/g BS /s, k_b = 0.0/h $m^{-1}s^{-1}$)	Adsorption or ion-exchange	R_6
CMW3+BS ↔ CB3 + BS (k_f = 0.00001 m^2/g BS /s, k_b = 0.0/h $m^{-1}s^{-1}$)	Adsorption or ion-exchange	R_7
CS1 ↔ CB1 (k_f = $Depo_1$/h g SS/m^3/s , k_b = $Eros_1$/h g BS/m^3/s)	Sedimentation	R_8
CS2 ↔ CB2 (k_f = $Depo_2$/h g SS/m^3/s , k_b = $Eros_2$/h g BS/m^3/s)	Sedimentation	R_9
CS3 ↔ CB3 (k_f = $Depo_3$/h g SS/m^3/s , k_b = $Eros_3$/h g BS/m^3/s)	Sedimentation	R_{10}
CMW1 ↔ CIMW1 (k_f = 0.00010$\theta^{T-15^\circ C}$ s^{-1}, k_b = 0.0$h_b\theta_b$/h$\theta^{T-15^\circ C}$ s^{-1}, θ = 1.2)	Diffusion	R_{11}
CMW2 ↔ CIMW2 (k_f = 0.00010$\theta^{T-15^\circ C}$ s^{-1}, k_b = 0.0$h_b\theta_b$/h$\theta^{T-15^\circ C}$ s^{-1}, θ = 1.2)	Diffusion	R_{12}
CMW3 ↔ CIMW3 (k_f = 0.00010$\theta^{T-15^\circ C}$ s^{-1}, k_b = 0.0$h_b\theta_b$/h$\theta^{T-15^\circ C}$ s^{-1}, θ = 1.2)	Diffusion	R_{13}
CIMW1+ CIMW2 ↔ CIMW3 (k_f = 0.002$h_b\theta_b$/h m^3/g /s, k_b = 0.005$h_b\theta_b$/h s^{-1})	Aqueous complexation	R_{14}
CIMW1+BS ↔ CB1 + BS (k_f = 0.00001$h_b\theta_b$/h m^2/g BS/s, k_b = 0.0/h /m/s)	Adsorption or ion-exchange	R_{15}
CIMW2+BS ↔ CB2 + BS (k_f = 0.00001$h_b\theta_b$/h m^2/g BS/s, k_b = 0.0/h /m/s)	Adsorption or ion-exchange	R_{16}
CIMW3+BS ↔ CB3 + BS (k_f = 0.00001$h_b\theta_b$/h m^2/g BS/s, k_b = 0.0/h /m/s)	Adsorption or ion-exchange	R_{17}
CMW2 ↔ P (k_f = 0.00002 /s, k_b = 0.02 g/m^3/ATM/s, P=0.0025ATM)	Volatilization	R_{18}
CMW3 ↔ SP3 (k_f = 0.0001 /s, k_b = 0.0000001 /s)	Precipitation/dissolution	R_{19}
CIMW3 ↔ BP3 (k_f = 0.0001 $h_b\theta_b$/h s^{-1}, k_b = 0.0000001 $h_b\theta_b$/h s^{-1})	Precipitation/dissolution	R_{20}

Initially, only bed sediments BS exist in the domain of interest with concentration of 50 g/m^2. As the simulation starts, in flow variable boundary conditions are applied to the upstream boundary sides, where all dissolved chemicals have a constant incoming concentration of 1 g/m^3 and all other mobile species and suspended sediment SS have zero incoming concentration. Out flow variable boundary conditions are applied to the downstream boundary sides. The longitudinal dispersivity is 10.0 m. A 12,000 second simulation is performed with fixed time step size of 200 seconds.

Figure 1 shows trend of increasing concentration of the suspended sediment along down stream direction. It indicates that deposition is less than erosion under the condition set for this example.
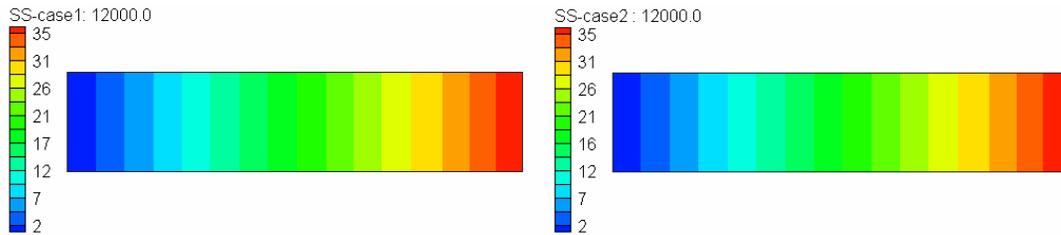

FIGURE 1. SS concentration (g/m^3) for example 3.1 (left: case 1 and right: case 2).

Figure 2 shows decreasing concentration of CMW1 along the downstream direction. This is because we allow the adsorption to happen, but do not allow desorption from particulate chemicals to dissolved chemicals to occur.
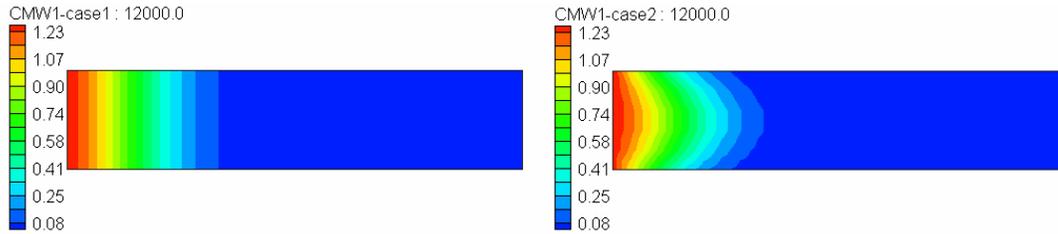

FIGURE 2. CMW1 concentration (g/m^3) for example 3.1 (left: case 1 and right: case 2).

Due to the temperature factor $\theta^{T-15°C}$ shown in Table 1, reaction rates of R_{11} through R_{13} increase 6.19 times as temperature increases from 15°C at the center of the domain to 25°C at the top and bottom edges for case 2. Increase of these reaction rates means more dissolved chemicals will diffuse from mobile water phase to immobile water phase, therefore, we observe greater CMW1 concentration at the center than at the edges in Figure 2.

3.2 Overland transport with eutrophication in QUAL2E

The Stream Water Quality Model QUAL2E (Brown and Barnwell, 1987) is a typical eutrophication model for stream systems. QUAL2E was first released in 1985 and has been successfully applied in many water quality studies since then.
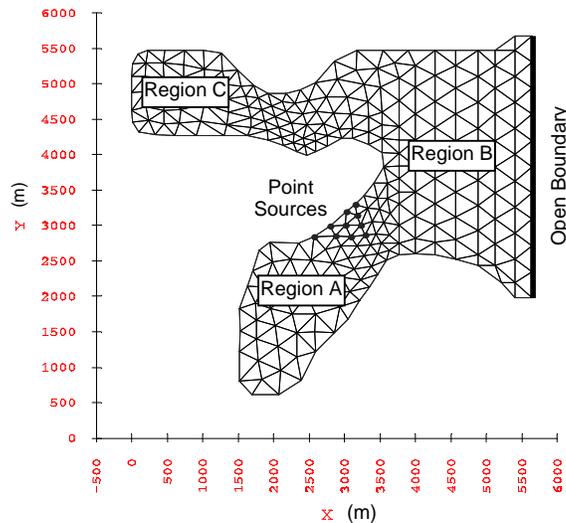

FIGURE 3. Simulation domain descretization for example 3.2.

As shown in Figure 3, the domain of interest is a shallow water body discretized with 462 elements and 275 nodes. Region A, B, and C are illustrated for simulation results discussion. The flow is allowed to reverse direction every 12 hours (T = 12 hours). The flow pattern was simulated using BEST2D (Yeh et al., 1998), with a flow-reversal boundary condition

implemented on the open boundary side and with the rest of the boundary treated as closed. It was also assumed subject to 10 point sources each with an injection rate of 1 m^3/s. The water depth varies from 0.7 m to 10.3 m during one flow-reversal cycle. The calculated flow velocity at various times during one flow-reversal cycle ranges from 0.02 m/s to 1.6 m/s.

To focus on transport, we assume that the temperature is 15°C throughout the simulation region. Variable boundary conditions are applied to the open boundary sides. Initial concentrations are O = 5 mg-O$_2$/kg, L = 0.8 mg-O$_2$/kg, Chl$\underline{a}$ = 20.0 μg-Chl$\underline{a}$/kg, N_4 = 2.0 mg-N/kg, N_1 = 1.0 mg-N/kg, N_2 = 0.1 mg-N/kg, N_3 = 1.0 mg-N/kg, P_1 = 0.5 mg-P/kg, and P_2 = 0.1 mg-P/kg. Variable boundary incoming concentrations of the 9 simulated species are 10% of their initial value. The dispersion coefficient was 5.2 m^2/s. Each point source injected the biochemical oxygen demand L at a rate of 20.0 g/m^2/s. A 30-day (60T) simulation is performed with a fixed time step size of 10 minutes.

Figure 4 plots the concentration contours of L and Chl$\underline{a}$ at different simulation time. It is seen that at the point sources, concentration of L increases due to the injection, and at the open boundary, concentration of L decreases due to the low incoming concentration. According to the reaction network of QUAL2E, the source of Chl$\underline{a}$ is algae growth, and the sink of Chl$\underline{a}$ includes algae respiration and settling. The Chl$\underline{a}$ concentration decrease indicates that the source is less than the sink. Because the settling rate of algae increases when water depth decreases, settling rate in region A is greater than in region C and settling rate in region C is greater than in region B. Therefore, we observe less Chl$\underline{a}$ concentration in region A than in region C and less Chl$\underline{a}$ concentration in region C than in region B. As the simulation time increases, when only small amount of Chl$\underline{a}$ is left, the concentration distribution is mainly affected by advective-dispersive transport rather than reactions.
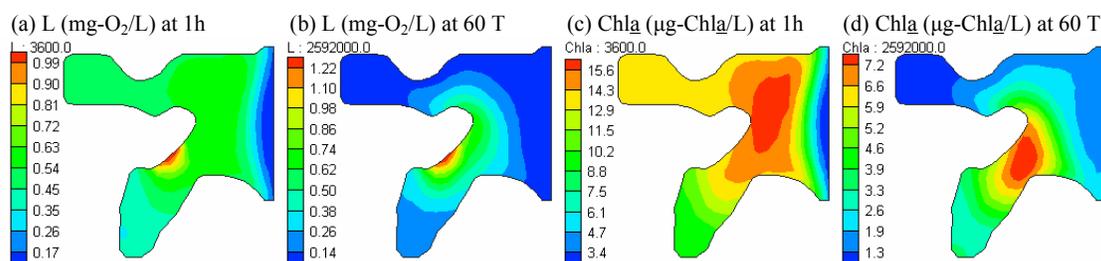

FIGURE 4. Concentration Contours for example 3.2.

In the original reports, there are 9 water quality state-variables related to eutrophication kinetics. In the context of reaction network, there are 16 biogeochemical reactions involving 19 constituents. All 16 rate equations depend only on the first 9 constituents; thus, the other 10 constituents can be decoupled from the first 9 in any simulation. Had evidence indicated that the rate formulation of the 16 kinetic reactions also depended on the other 10 constituents in a system, all 19 constituents should have been modeled simultaneously. The important question then is what we should do to calibrate the model. A general paradigm is developed that provides a protocol for formulating the rates of reactions and discovering the assumptions and limitations of the model employed.

Substitution of the reaction network for QUAL2E into equation (5) results in 19 ordinary differential equations for 19 species in a well-mixed system. In a "true" reaction-based approach, governing equations for all species involved in the reaction network must be considered. The diagonalization of the reaction matrix for all 19 species would result in a set

of 15 kinetic-variable equations [equations (1) through (9) and (14) through (19) in Table 2] and 4 component equations [equations (10) through (13) in Table 2].

The use of diagonalization approaches allows one to formulate some rate equations one by one. For example, the reaction rate R_8 can be calculated by plotting the concentration of E_7 versus time in which E_7 is the linear combination of C_3, C_4, C_5, C_6, C_7, $Chla_{(b)}$ and $P_{2(b)}$ [see equation (7) in Table 2]. Similarly, reaction rates R_{11}, R_{13}, R_4, R_6, R_{12}, R_{14}, R_{15}, and R_{16} can be calculated from the dynamics of E_8 through E_{15}, respectively [see equations (8), (9) and (14) through (19) in Table 2]. Because linearly dependent reactions are present in the system, one cannot formulate all rate equations independently. To do so, one has to design an experimental system such that only linearly independent reactions are present to individually and mechanistically formulate rate equations.

TABLE 2. Governing equations for the reaction-based diagonalization approach.

Decomposition Equations	No.
$dE_1/dt = d\left[0.00027\left(C_3 + Chla_{(b)}\right) + C_9 + P_{2(b)}\right]\Big/dt = -0.015R_3 + R_{10}$	1
$dE_2/dt = d\left[C_9 + P_{2(b)}\right]\Big/dt = -0.015R_1 + R_{10}$	2
$dE_3/dt = d\left[-0.21\left(C_1 - C_2 + O_{2(g)} + O_{(b)} - L_{(b)}\right) + 0.0078\left(C_3 + Chla_{(b)}\right) - 0.77C_6 - C_7 + 5.1\left(C_9 + P_{2(b)}\right)\right]\Big/dt = R_2 + 5.1R_{10}$	3
$dE_4/dt = d\left[0.00032\left(C_3 + Chla_{(b)}\right) + 0.22\left(C_4 + N_{4(b)}\right) + 1.2\left(C_9 + P_{2(b)}\right)\right]\Big/dt = -0.22R_5 + 1.2R_{10}$	4
$dE_5/dt = d\left[-0.22\left(C_1 - C_2 + O_{2(g)} + O_{(b)} - L_{(b)}\right) + 0.0078\left(C_3 + Chla_{(b)}\right) + 0.23C_6 + 5.1\left(C_9 + P_{2(b)}\right)\right]\Big/dt = R_7 + 5.11R_{10}$	5
$dE_6/dt = d\left[0.0094\left(C_1 - C_2 + O_{2(g)} + O_{(b)}\right) - 0.00033\left(C_3 + Chla_{(b)}\right) + 0.033C_6 - 0.22\left(C_9 + P_{2(b)}\right)\right]\Big/dt = -0.043R_9 - 0.22R_{10}$	6
$dE_7/dt = d\left[0.0015\left(C_3 + Chla_{(b)}\right) + C_4 + C_5 + C_6 + C_7 + N_{4(b)}\right]\Big/dt = R_8$	7
$dE_8/dt = d\left[0.00027\left(C_3 + Chla_{(b)}\right) + C_8 + C_9 + P_{2(b)}\right]\Big/dt = -R_{11}$	8
$dE_9/dt = d\left(C_2 + L_{(b)}\right)\Big/dt = -R_{13}$	9
$dT_1/dt = d\left(C_2 + L_{(b)} + H_2O\right)\Big/dt = 0$	10
$dT_2/dt = d\left(C_2 + L_{(b)} + CO_2\right)\Big/dt = 0$	11
$dT_3/dt = d\left[0.0015\left(C_3 + Chla_{(b)}\right) + C_4 + C_5 + C_6 + C_7 + N_{1(b)} + N_{4(b)}\right]\Big/dt = 0$	12
$dT_4/dt = d\left[0.00027\left(C_3 + Chla_{(b)}\right) + C_8 + C_9 + P_{1(b)} + P_{2(b)}\right]\Big/dt = 0$	13
$dE_{10}/dt = dChla_{(b)}\Big/dt = R_4$	14
$dE_{11}/dt = dN_{4(b)}\Big/dt = R_6$	15
$dE_{12}/dt = dP_{2(b)}\Big/dt = -R_{12}$	16
$dE_{13}/dt = dL_{(b)}\Big/dt = R_{14}$	17
$dE_{14}/dt = dO_{2(g)}\Big/dt = -R_{15}$	18
$dE_{15}/dt = dO_{(b)}\Big/dt = R_{16}$	19

Note: $C_1 = O$, $C_2 = L$, $C_3 = Chl\underline{a}$, $C_4 = N_4$, $C_5 = N_1$, $C_6 = N_2$, $C_7 = N_3$, $C_8 = P_1$, and $C_9 = P_2$

4. SUMMARY

This paper presents the development of a numerical model for transient simulation of sediment and biogeochemical species as they are transported in the overland shallow water of watershed systems. Transport equations based on the principle of mass balance are used to describe temporal-spatial distributions of sediments and water qualities. Biochemical and geochemical processes are completely defined with reaction network and dealt with reaction-based approaches. Through the decomposition of the system of species transport equations, kinetic-variables rather than individual species are considered as primary dependent variables and linearly independent reaction can be measured by a kinetic variable.

5. ACKNOWLEGEMENTS

REFERENCES

- Ambrose, R.B., Wool, T.A., and Martin, J.L., 1993. The Water Quality Analysis Simulation Program, WASP5 Part A: Model Documentation. Environmental Research Laboratory, US Environmental Protection Agency, Athens, GA.
- Bonnet, M. P. and Wessen, K., 2001. ELMO, a 3-D water quality model for nutrients and chlorophyll: first application on a lacustrine ecosystem. Ecological Modeling, 141(1-3): 19-33.
- Brown, L.C., and Barnwell, T.O., 1987. The Enhanced Stream Water Quality Models QUAL2E and QUAL2E-UNCAS: Documentation and User Manual. US Environmental Protection Agency, Report No. EPA/600/3–87/007.
- Cerco, C.F., and Cole, T., 1995. User's Guide to the CE-QUAL-ICM Three-Dimensional Eutrophication Model, Release Version 1.0. Technical Report EL-95-15, US Army Engineer Waterways Experiment Station, Vicksburg, MS, 1995.
- Fang, Y. L., Yeh, G. T. and Burgos W. D., 2003. A Generic Paradigm to Model Reaction-Based Biogeochemical Processes in Batch Systems. Water Resources Research 33(4): 1083-1118.
- Gerritsen, H., Vos, R.J., Kaaij, T., Laneand A., and Boon, J.G., 2000. Suspended sediment modeling in a shelf sea (North Sea). Coastal Engineering, 41:317-352
- Prandle, D., Hargreaves, J.C., McManus, J.P., Campbell, A.R., Duwe, K., Lane, A., Mahnke, P., Shimwell, S., and Wolf, J., 2000. Tide, wave and suspended sediment modeling on an open coast − Holderness. Coastal Engineering, 41: 237-267 .
- Shen, Y., Zheng, Y., Komatsu, T., and Kohashi, N., 2002. A three-dimensional numerical model of hydrodynamics and water quality in Hakata Bay. Ocean Engineering, 29 (4): 461-473.
- Steefel, C. I., and Cappellen, V.P., 1998. Preface: Reactive transport modeling of natural systems. J. Hydrol. 209: 1–7.
- Yeh, G. T., Cheng, H. P., and Cheng, J. R., 1998. BEST: A Numerical Model to Simulate Bay/Estuarine Hydrodynamics and Sediment-chemical Transport. Technical Report to National Association of Steel and Shipbuilding Companies. Department of Civil and Environmental Engineering, The Pennsylvania State University, University Park, PA 16802.
- Yeh, G. T., Huang, G. B., Cheng, H. P., and Zhang, F., 2005. Chapter 9, A First-Princeple, Phusics-Based Watershed Model: WASH123D. Watershed Models.
- Zheng, L., Chen, C. and Zhang, F.Y., 2004. Development of water quality model in the Satilla River Estuary, Georgia. Ecological Modelling, 178 (3-4): 457-482.